

Genesis and trends in marine heatwaves over the tropical Indian Ocean and their interaction with the Indian summer monsoon

J. S. Saranya^{1,2}, M K Roxy^{1*}, Panini Dasgupta^{1,3} and Ajay Anand^{1,4}

¹*Centre for Climate Change Research, Indian Institute of Tropical Meteorology, Pune 411008, India*

²*Academy of Climate Change Education and Research, Kerala Agricultural University, Kerala, 680656, India*

³*Department of Meteorology and Oceanography, College of Science and Technology, Andhra University, Visakhapatnam, Andhra Pradesh 530003, India*

⁴*Department of Atmospheric Sciences, Cochin University of Science and Technology, Kerala, 682022, India*

*Corresponding author address: Roxy Mathew Koll, Indian Institute of Tropical Meteorology, Pune 411008, India.
E-mail: roxy@tropmet.res.in

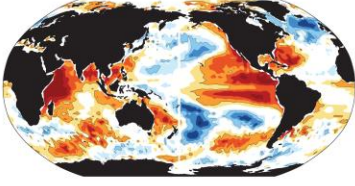
Contents of this file

Figures S1 to S7

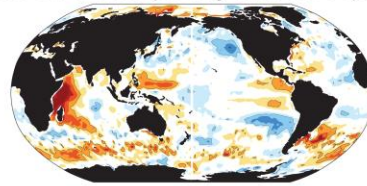
Correlation: MHW days and SST

Correlation: MHW frequency and SST

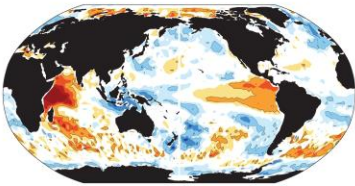
a WIO MHW days and SST (annual)



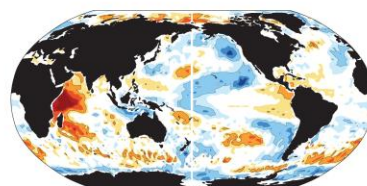
b WIO MHW frequency and SST (annual)



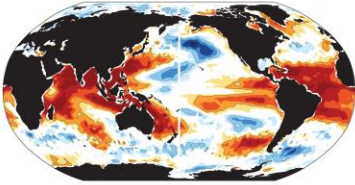
c WIO MHW days and SST



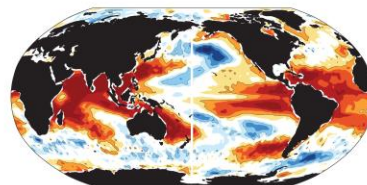
d WIO MHW frequency and SST



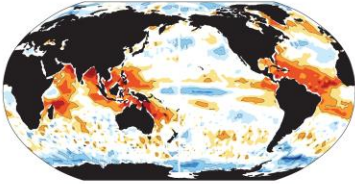
e BoB MHW days and SST (annual)



f BoB MHW frequency and SST (annual)



g BoB MHW days and SST



h BoB MHW frequency and SST

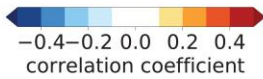
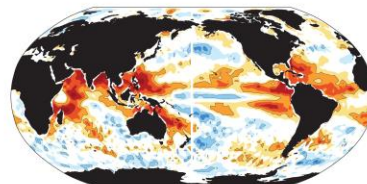


Figure S1: Correlation map between the total number of MHW days and global SST for annual (a, e) and June to September (c, g) in the western Indian Ocean (WIO) and the north Bay of Bengal (BoB). (B) Correlation map between the total number of MHW events and global SST for annual (b, f) and June to September (d, h) in the western Indian Ocean (WIO) and the north Bay of Bengal (BoB).

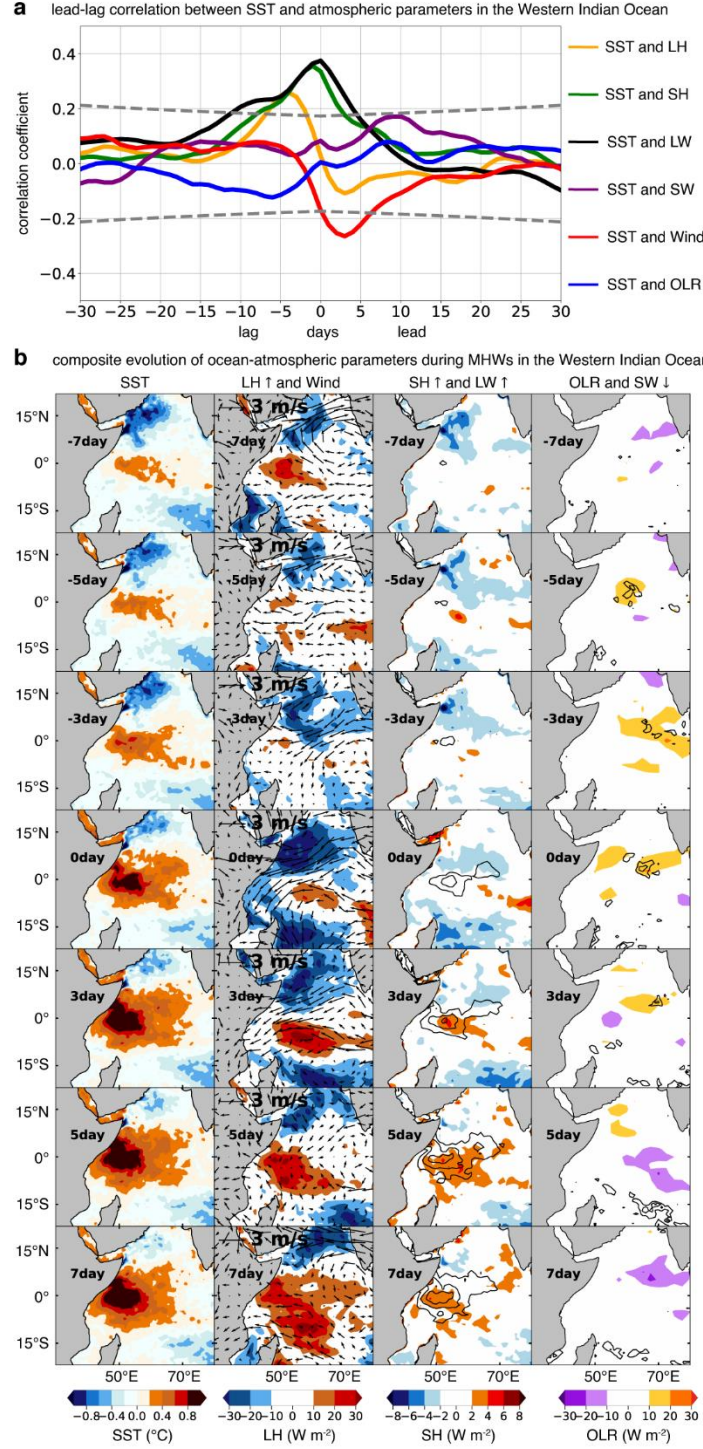


Figure S2: (a) The lead-lag correlation between SST and wind speed (red line), latent heat flux (orange line), sensible heat flux (green line), upward long wave radiation (black line), OLR (blue line) in the western Indian Ocean, estimated from the 30 days before and 30 days after the genesis of MHW events. The dotted lines represent the 95% confidence level. Composite evolution of (b) SST ($^{\circ}\text{C}$), latent heat (LH, W m^{-2}), wind (m s^{-1}), OLR (W m^{-2}), shortwave radiation (SW, W m^{-2}), sensible heat (SH, W m^{-2}), and longwave (LW, W m^{-2}), in the western Indian Ocean before and during MHWs for the period 1982–2018, using ERA5 reanalysis datasets. Upward arrow represents the exchange of flux from ocean to atmosphere and downward arrow represents the exchange of flux from ocean to atmosphere.

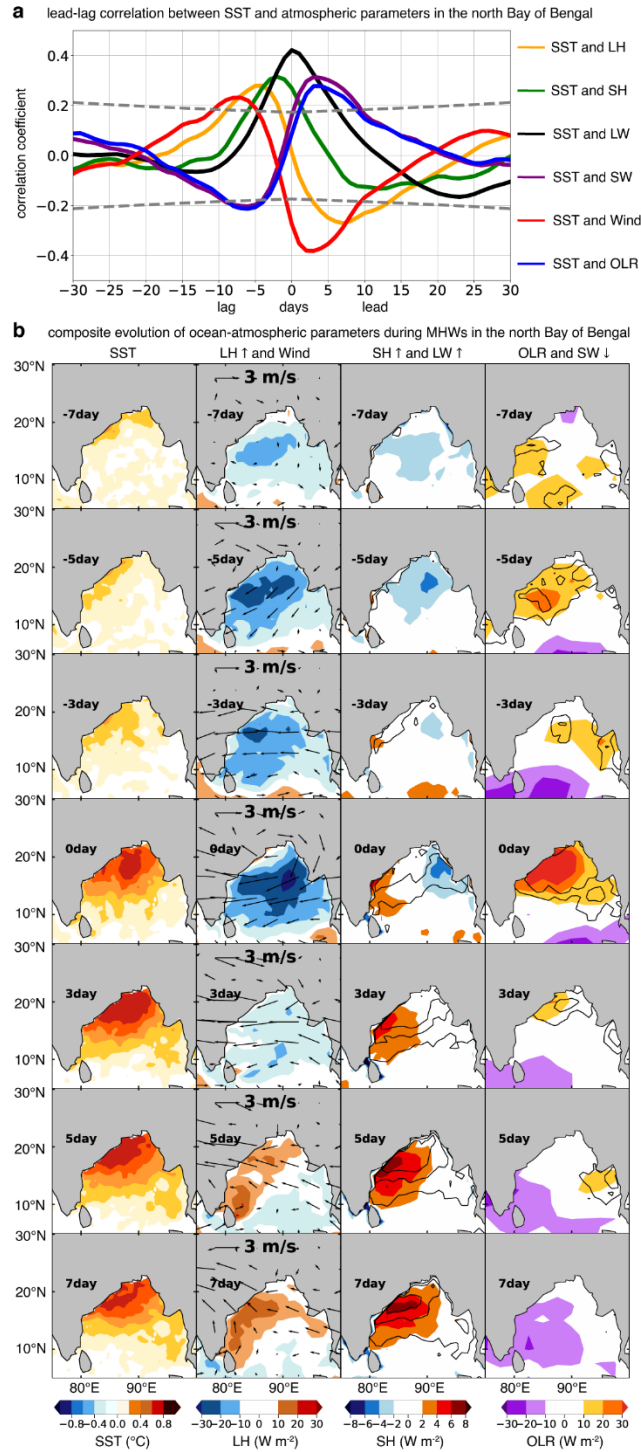


Figure S3: (a) The lead-lag correlation between SST and wind speed (red line), latent heat flux (orange line), sensible heat flux (green line), upward long wave radiation (black line), OLR (blue line) in the north Bay of Bengal, estimated from the 30 days before and 30 days after the genesis of MHW events. The dotted lines represent the 95% confidence level. Composite evolution of (b) SST ($^{\circ}\text{C}$), latent heat (LH, W m^{-2}), wind (m s^{-1}), OLR (W m^{-2}), shortwave radiation (SW, W m^{-2}), sensible heat (SH, W m^{-2}), and longwave (LW, W m^{-2}), in the western Indian Ocean before and during MHWs for the period 1982–2018, using ERA5 reanalysis datasets. Upward arrow represents the exchange of flux from ocean to atmosphere and downward arrow represents the exchange of flux from ocean to atmosphere.

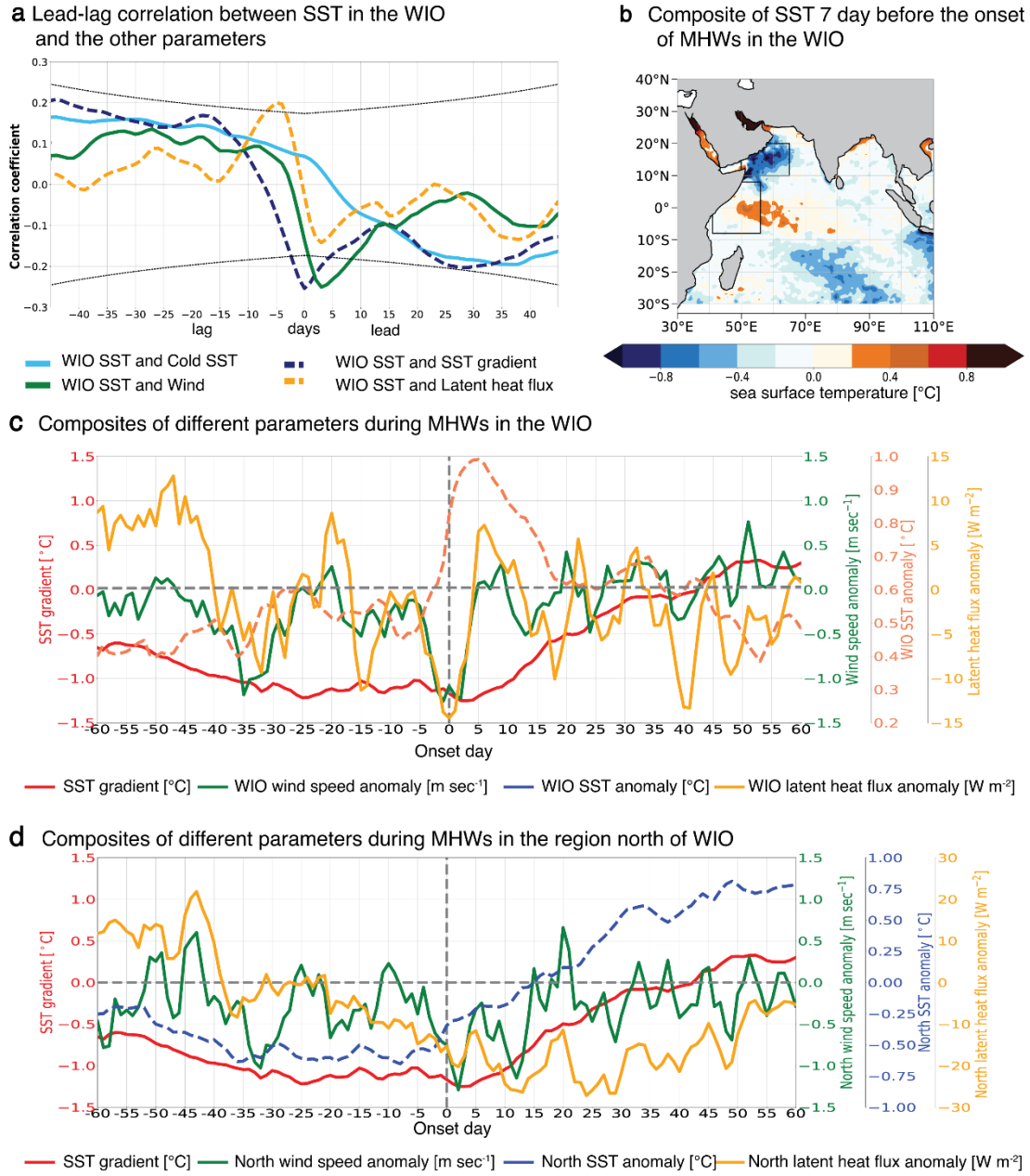


Figure S4: (a) Lead-lag correlation between SST anomalies in the western Indian Ocean (WIO) and SST anomalies at (i) north box, (ii) north-south SST gradient, (iii) wind speed over WIO, and (iv) latent heat flux over WIO. (b) composite of SST 7 days before the onset of MHWs in the WIO, (c) composites of i, ii, iii, and iv at WIO, and (d) composite of i, ii, iii, and iv at the region north of WIO, during -60 to 60 days centering the onset date.

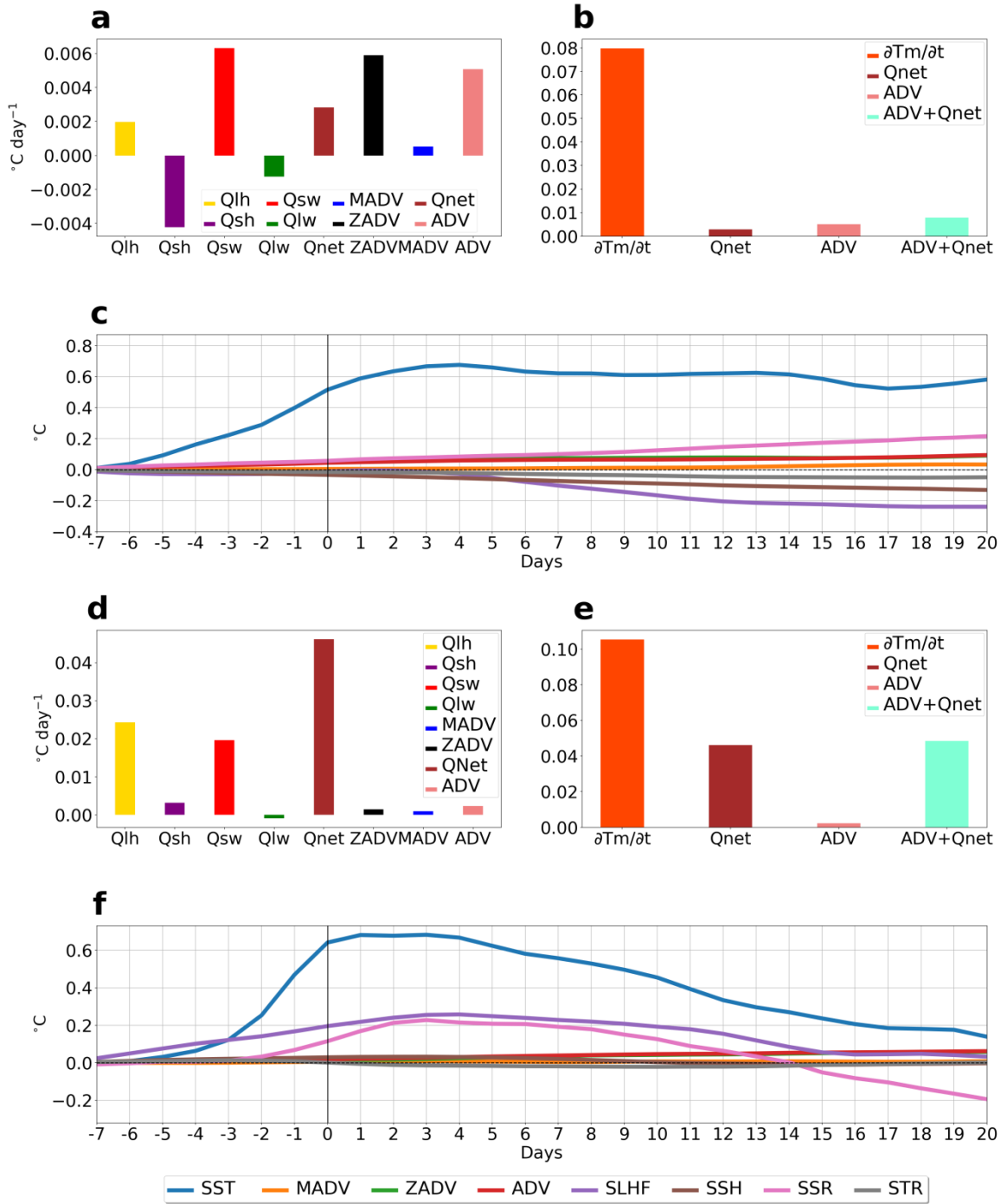


Figure S5: The heat budget terms calculated for the 5 days before the starting date of MHW in the western Indian Ocean (41°E–56°E, 8°S–8°N) region, (a) terms in the right-hand side of the temperature tendency equation, (b) terms in both side of the temperature tendency equation (in $^{\circ}\text{C day}^{-1}$), (c) the line plot of time integrated heat budget terms (in $^{\circ}\text{C}$). The heat budget terms calculated for the 5 days before the starting date of MHW in the north Bay of Bengal (85°E–93°E, 15°N–23°N) region, (d) terms in the right-hand side of the temperature tendency equation, (e) terms in both side of the temperature tendency equation (in $^{\circ}\text{C day}^{-1}$), (f) line plot of time integrated heat budget terms (in $^{\circ}\text{C}$). Using the OSCAR hydrographic datasets and ERA5 heat fluxes from 1994 to 2015.

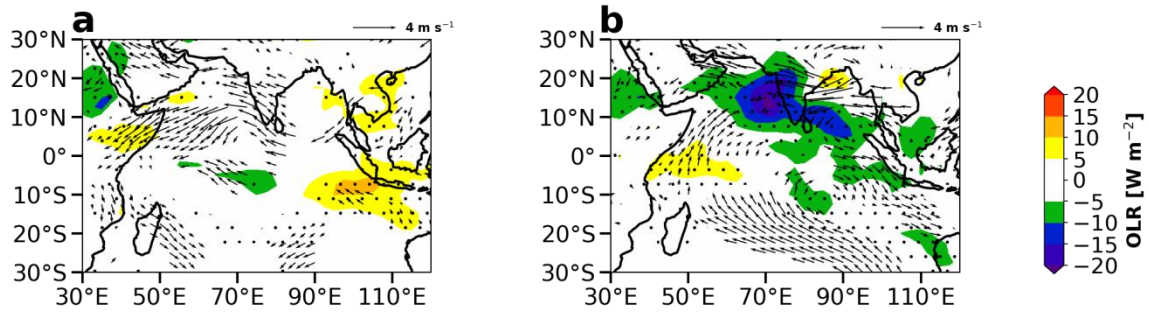


Figure S6: The circulation anomalies at 850 hPa (in m s^{-1}) and Outgoing Long wave Radiation (OLR) anomalies (in W m^{-2}) for MHW days (a) in the WIO (41°E–56°E, 8°S–8°N) region and (b) in north Bay of Bengal (85°E–93°E, 15°S–23°N) region during June–September from 1982–2018. Dots and vectors represent 95% confidence level.

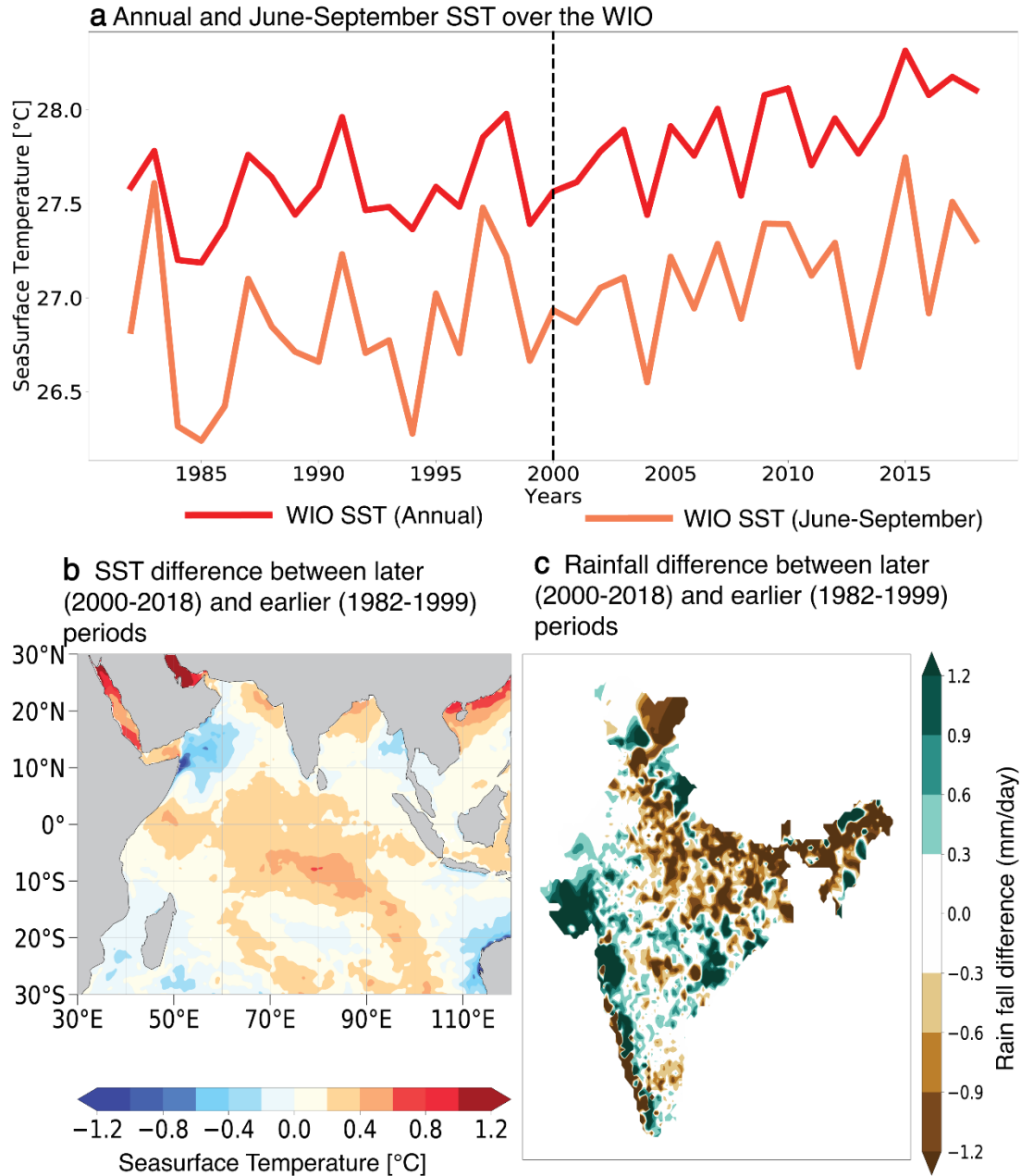


Figure S7: (a) Annual and June-September SST over the western Indian Ocean (WIO), (b) SST difference between later (2000–2018) and earlier (1982–1999) periods (June to September), (c) Rainfall difference between later (2000–2018) and earlier (1982–1999) periods (June to September).